Statistics and Its Interface Volume 10 (2017) 575–584

EWMA control charts for multivariate autocorrelated processes*

Yuhui Chen†,‡

In this paper, a semiparametric control scheme for multivariate Markov processes of order *one* is introduced. We utilize copula-based semiparametric stationary Markov models to transform original multivariate autocorrelated processes to the ones in which the marginal information of the monitored characteristics are separate out from their dependence structures. Meanwhile, the autocorrelations within them are also characterized by copulas. As such, one could focus on monitoring changes in the location of characteristics marginally under a more generalized assumption that observations could be stochastically dependent. The proposed chart can reduce to the traditional multivariate EWMA charts if the underlying process is multivariate Gaussian with stochastically independent observations. In addition, the margin of each time series is fitted by a newly developed semiparametric approach using the transformed Bernstein polynomial prior. Specifically, it allows an initial parametric guess (such as normal) on a monitored characteristic; then by adding more details via data, any departure from this initial guess will be captured and used for adjusting the initial to obtain robust estimation. Gaussian copulas are then used for modeling both autocorrelations within each time series and correlations among them.

Keywords and phrases: Autocorrelated processes, Gaussian copulas, Multivariate EWMA charts, Semiparametric models, Transformed Bernstein polynomial priors.

1. INTRODUCTION

Recently, the statistical process control (SPC) tool has become more and more important not only in the area of quality monitoring but also in many other fields of science, economics, and medicine. Traditional charts used to monitor a single quality characteristic are typically constructed by three major control schemes, i.e., the Shewhart charts (Shewhart, 1931; Duncan, 1965), the CUSUM charts (Page, 1954; Hawkins and Olwell, 1998), and the EWMA charts (Roberts, 1959; Crowder, 1987; Crowder, 1989; Lucas and Saccucci, 1990). To further relax the normality assumption on the traditional charts, many nonparametric charts thus were proposed for better monitoring non-Gaussian processes, see Willemain and Runger (1996), Albers and Kallenberg (2004), Chakraborti and Eryilmaz (2007), Ross and Adams (2012), and Chen (2015). However, the rapids growth of data acquisition technology and the use of powerful computers for quality control have led to an interest in simultaneously monitoring several quality characteristics. To this point, multivariate control schemes, such as the Hotelling T^2 charts (Hotelling, 1947), the multivariate CUSUM charts (Woodall and Ncube, 1985; Crosier, 1988; Pignatiello and Runger, 1990; Tartakovsky, 2014), and the multivariate EWMA charts (Lowry et al., 1992), have been proposed to take advantage of the relationships among the monitored characteristics. Particularly, the multivariate EWMA chart is received more attention due to its sensitivity to small and moderate shifts in the location. Chen et al. (2016+) borrowed the idea of the multivariate EWMA charts and thus constructed the multivariate nonparametric charts using weighted Polya trees (Hanson, 2006; Chen and Hanson, 2014) for quickly detecting the change points for either multivariate Gaussian or non-Gaussian processes.

However, all of those attempts were derived under the assumption that observations are stochastically independent. In some areas, characteristics are measured in the time order of the production, such as the areas in medicine and in economics. It is well known that even with a mild violation on the independence assumption, the traditional charts may signal incorrectly and weaken the effectiveness of detecting shifts. To this point, Chan and Li (1994) and Charnes (1995) presented extensions of multivariate Shewhart charts to account for both autocorrelations within characteristics and correlations across them. Chen and Hanson (2016+) used a newly developed transformed Bernstein polynomial prior (Chen et al., 2014) to construct nonparametric regression charts by integrating the extra monitored characteristics as the covariates into regression models, and thus the charts can better monitor the single key characteristic adjusted by those external covariates. Alwan and Roberts (1988), Montgomery and Mastrangelo (1991), and Lu and Reynolds (1995) instead introduced the charts constructed by independent residuals. However, if the model is not adequate for the monitored process, the residuals may not be independent, and consequently, nuisance alarms will be triggered. To solve this issue, Kalgonda and Kulkarni (2004) proposed

*This research was supported in part by Research Grants Committee, University of Alabama.
†Assistant Professor, Department of Mathematics, The University of Alabama.
‡To whom all correspondence should be addressed: ychen164@ua.edu.

a multivariate quality control chart for directly monitoring the mean of an autocorrelated process in which observations can be modeled as a VAR(1) process under the normality assumption. For other literatures of multivariate sequential charts, see Theodossiou (1993), Kramer and Schmid (1997), Moskvina and Zhigljavsky (2003), and Martin and Petr (2012).

The aim of this paper is to propose a multivariate semiparametric control scheme to monitor autocorrelated multivariate processes via transformation from a class of copula-based semiparametric stationary Markov models. The key advantage of the proposed method is to separate out the marginal information of the monitored characteristics from their dependence structures, and the dependencies characterized by copulas are invariant to any increasing transformation of the times series. As such, one could focus on monitoring marginal changes in the location of characteristics (usually the common interest of quality control) under a more generalized assumption that observations could be stochastically dependent. Moreover, by transforming an original autocorrelated process upon Gaussian copulas, the transformed Markov process has its white noises normally distributed. Consequently, with the normal assumption on all margins, this proposed chart performs in a similar way to the multivariate EWMA chart which assumes AR(1) process with randomly normally distributed errors. With an additional assumption that the autocorrelations do not exist for all characteristics, this chart further reduces to the traditional multivariate EWMA chart with the estimated chart parameters. To monitor Gaussian or non-Gaussian distributed characteristics marginally, we utilize a newly developed semiparametric prior called the transformed Bernstein polynomial prior (Chen et al., 2014). This new method allows an initial parametric guess (or centering parametric distribution) on a monitored characteristic, such as normal; then by adding more details via data, any departure from this initial guess will be captured and used for adjusting the initial to obtain robust estimations. Gaussian copulas are then used for evaluating the dependence structure among the characteristics and their autocorrelations as well. Other copulas also could be used such as Student-t copulas for the both lower and upper tail dependence, Clayton copulas for the lower tail dependence, and Gumbel copulas for the upper tail dependence. However, in this paper, we only consider the Gaussian copulas since this dependence structure is the common assumption on multivariate processes.

The rest of the paper is organized as follows. In Section 2, we introduce multivariate Gaussian copula Markov processes of order *one*, and in Section 3 we construct semiparametric multivariate EWMA control charts based on the transformed Gaussian copula Markov processes. We further present the estimation procedure for the proposed charts in Section 4. Simulation studies are then conducted in Section 5 for both multivariate Gaussian or non-Gaussian underlying Markov processes. An example is illustrated in Section 6 with comparison to other existing multivariate control schemes. Conclusions are given in Section 7.

2. MULTIVARIATE GAUSSIAN COPULA MARKOV PROCESSES OF ORDER ONE

Let consider d stationary univariate Markov processes of order *one*, $\{X_{t,s}, t \in \mathcal{Z}^+\}$ for $s = 1, 2, \ldots, d$ and $\mathcal{Z}^+ = \{1, 2, 3, \ldots\}$, with continuous state space. By Sklar's theorem (1959), for each time series $\{X_{t,s}\}$, the joint distribution of $X_{t-1,s}$ and $X_{t,s}$ can be expressed in terms of the marginal distribution of $X_{t,s}$, denoted as $G_s(\cdot)$, and the copula function $C_s(\cdot,\cdot)$ of $X_{t-1,s}$ and $X_{t,s}$ uniquely. With the **assumption** (Chen and Fan, 2006): $\{X_{t,s} : t \in \mathcal{Z}^+\}$, for $s = 1, 2, \ldots, d$, is a sample of a stationary first-order Markov process generated from $(G_s(\cdot), C_s(\cdot,\cdot))$, where $G_s(\cdot)$ is the true invariant distribution which is absolutely continuous with respect to Lebesgue measure on the real line, and $C_s(\cdot,\cdot)$ is the true parametric copula of $X_{t,s}$ and $X_{t-1,s}$, which is absolutely continuous with respect to Lebesgue measure on $[0,1]^2$ and is neither the Fréchet-Hoeffding upper nor lower bound, then the transformed process, $\{U_{t,s} : U_{t,s} = G_s(X_{t,s})\}$, is also a stationary Markov process of order *one* with the joint distribution of $U_{t,s}$ and $U_{t-1,s}$ given by $C_s(u_{t,s}, u_{t-1,s})$ and the conditional density of $U_{t,s}$ given $U_{t-1,s}$ is $f_{U_{t,s}|U_{t-1,s}=u^*_{t-1,s}} = c_s(u_{t,s}, u^*_{t-1,s})$, where $c_s(\cdot,\cdot)$ is the copula density associated with $C_s(\cdot,\cdot)$. It implies that the assumption is consistent with the *generalized regression transformation* model (Chen and Fan, 2006):

$$H(G_s(X_{t,s})) = H(G_s(X_{t-1,s})) + \epsilon_{t,s}, \quad \text{for } s = 1, 2, \ldots, d, \tag{1}$$

where $E(\epsilon_{t,s}|X_{t-1,s}) = 0$, $G_s(\cdot)$ is the true unknown distribution function of $X_{t,s}$, and $H(\cdot)$ is a parametric increasing function. Further, by assuming a Gaussian copula of $X_{t-1,s}$ and $X_{t,s}$, the process $\{X_{t,s}\}$ from Eq. (1) then satisfies

$$\begin{aligned} &\Phi^{-1}(G_s(X_{t,s})) \\ &\quad = \rho_s \Phi^{-1}(G_s(X_{t-1,s})) + \epsilon_{t,s}, \quad \text{for } s = 1, 2, \ldots, d, \end{aligned} \tag{2}$$

where Φ^{-1} is the quantile function of the standard normal, ρ_s is the Gaussian copula parameter, and $\epsilon_{t,s} \sim N(0, 1-\rho_s^2)$ independent of $X_{t-1,s}$.

Let $Y_{t,s} = \Phi^{-1}(G_s(X_{t,s}))$ and $Y_{t-1,s} = \Phi^{-1}(G_s(X_{t-1,s}))$, Eq. (2) is then rewritten as

$$Y_{t,s} = \rho_s Y_{t-1,s} + \epsilon_{t,s}, \quad \text{for } s = 1, 2, \ldots, d. \tag{3}$$

Following the discussion in Chen and Fan (2006), $\{Y_{t,s}, t \in \mathcal{Z}^+\}$, for $s = 1, 2, \ldots, d$, is a stationary Gaussian Markov process of order *one* with $E(Y_{t,s}) = 0$ and $Var(Y_{t,s}) = \frac{1-\rho_s^2}{1-\rho_s^2} = 1$. By allowing $G_s(\cdot)$ to be a non-Gaussian distribution, Eq. (3) can be used to fit a stationary Markov process of order *one* with the Gaussian copula and any non-Gaussian marginal distribution. By noting that $Y_{t,s}|Y_{t-1,s} \sim N(\rho_s Y_{t-1,s}, 1-\rho_s^2)$, we could obtain

$$(4) \qquad \begin{pmatrix} Y_{t-1,s} \\ Y_{t,s} \end{pmatrix} \sim N\left(\begin{pmatrix} 0 \\ 0 \end{pmatrix} \begin{pmatrix} 1 & \rho_s \\ \rho_s & 1 \end{pmatrix} \right).$$

Further, in order to consider the correlations among those time series, let us define

$$(5) \qquad \mathbf{Y}_t = \mathbf{\Delta}\mathbf{Y}_{t-1} + \boldsymbol{\epsilon}_t,$$

where $\mathbf{Y}_t = (Y_{t,1}, \ldots, Y_{t,d})'$, $\mathbf{Y}_{t-1} = (Y_{t-1,1}, \ldots, Y_{t-1,d})'$, and $\boldsymbol{\epsilon}_t = (\epsilon_{t,1}, \ldots, \epsilon_{t,d})'$ are $d \times 1$ vectors. $\mathbf{\Delta}$ is a $d \times d$ diagonal matrix with $\mathbf{\Delta} = \text{diag}(\rho_1, \rho_2, \ldots, \rho_d)$, which implies that each time series depends *only* upon its own lags and not on lags of another time series. We further assume that the correlation matrix and covariance matrix for $\boldsymbol{\epsilon}_t$ are consistent with the time t, thus denoted as $\mathbf{\Omega}_{\boldsymbol{\epsilon}}$ and $\mathbf{\Sigma}_{\boldsymbol{\epsilon}}$ respectively, we then have $\boldsymbol{\epsilon}_t \overset{i.i.d.}{\sim} N_d(\mathbf{0}, \mathbf{\Sigma}_{\boldsymbol{\epsilon}})$. Accordingly, the multivariate process $\{\mathbf{Y}_t, t \in \mathcal{Z}^+\}$ defined in Eq. (5) is a (weakly) stationary multivariate Gaussian Markov process of order *one* with the mean, $\boldsymbol{\mu}_{\mathbf{Y}} = \mathbf{0}$, and the auto-covariance matrix at lag h, $\mathbf{\Sigma}_{\mathbf{Y}}(h) = Cov(\mathbf{Y}_t, \mathbf{Y}_{t-h}) \overset{def.}{=} [\omega_{i,j}(h)]_{i,j=1}^{d}$. For $i \neq j$, $\omega_{i,j}(h)$ measures the cross-covariance of the two series $\{Y_{t,i}\}$ and $\{Y_{t-h,j}\}$. In addition, by the stationary property, we have $\mathbf{\Sigma}_{\boldsymbol{\epsilon}} = \mathbf{\Sigma}_{\mathbf{Y}}(0) - \mathbf{\Delta}\mathbf{\Sigma}_{\mathbf{Y}}(0)\mathbf{\Delta}'$. For a bivariate process, for example, by assuming

$$\mathbf{\Omega}_{\boldsymbol{\epsilon}} = \begin{pmatrix} 1 & \rho_r \\ \rho_r & 1 \end{pmatrix}$$

implies

$$(6) \quad \mathbf{\Sigma}_{\boldsymbol{\epsilon}} = \begin{pmatrix} 1-\rho_1^2 & \rho_r\sqrt{(1-\rho_1^2)(1-\rho_2^2)} \\ \rho_r\sqrt{(1-\rho_1^2)(1-\rho_2^2)} & 1-\rho_2^2 \end{pmatrix},$$

we obtain

$$\begin{aligned} \mathbf{\Sigma}_{\mathbf{Y}}(0) &= Cov(\mathbf{Y}_t, \mathbf{Y}_t) \\ &= \begin{pmatrix} 1 & \frac{\rho_r\sqrt{(1-\rho_1^2)(1-\rho_2^2)}}{(1-\rho_1\rho_2)} \\ \frac{\rho_r\sqrt{(1-\rho_1^2)(1-\rho_2^2)}}{(1-\rho_1\rho_2)} & 1 \end{pmatrix}. \end{aligned}$$

In addition, the auto-covariance matrix for the model in Eq. (5) at lag $h \geq 0$ satisfies

$$(7) \qquad \mathbf{\Sigma}_{\mathbf{Y}}(h) = Cov(\mathbf{Y}_t, \mathbf{Y}_{t-h}) = \mathbf{\Delta}^h\mathbf{\Sigma}_{\mathbf{Y}}(0),$$

and

$$(8) \qquad \mathbf{\Sigma}_{\mathbf{Y}}(-h) = Cov(\mathbf{Y}_{t-h}, \mathbf{Y}_t) = \mathbf{\Sigma}_{\mathbf{Y}}(0)\mathbf{\Delta}^h.$$

3. SEMIPARAMETRIC MULTIVARIATE EWMA CONTROL CHARTS FOR MONITORING GAUSSIAN OR NON-GAUSSIAN MARKOV PROCESSES

Let $\{\mathbf{X}_t : \mathbf{X}_t = (X_{t,1}, \ldots, X_{t,d})', t \in \mathcal{Z}^+\}$ and $\{\mathbf{X}_t^* : \mathbf{X}_t^* = (X_{t,1}^*, \ldots, X_{t,d}^*)', t \in \mathcal{Z}^+\}$ be in-control target and actually observed Markov processes, respectively. Further, let $\{\mathbf{Y}_t : \mathbf{Y}_t = (Y_{t,1}, \ldots, Y_{t,d})', t \in \mathcal{Z}^+\}$ and $\{\mathbf{Y}_t^* : \mathbf{Y}_t^* = (Y_{t,1}^*, \ldots, Y_{t,d}^*)', t \in \mathcal{Z}^+\}$ be the transformed Gaussian Markov processes from $\{\mathbf{X}_t\}$ and $\{\mathbf{X}_t^*\}$ (see Eq. (2), Eq. (3), Eq. (4), and Eq. (5)), respectively, with $Y_{t,s} = \Phi^{-1}(G_s(X_{t,s}))$ and $Y_{t,s}^* = \Phi^{-1}(G_s(X_{t,s}^*))$ for $s = 1, \ldots, d$, where $G_s(\cdot)$ is the true margin for the in-control process $\{X_{t,s}\}$. In practice, it will be estimated in Phase I using the method in Section 4.

As usual, we use a multivariate EWMA control scheme to detect the changes in the location for multivariate Markov processes, and thus the chart statistic is given by

$$(9) \qquad \mathbf{Z}_t = (I - \Lambda)\mathbf{Z}_{t-1} + \Lambda\mathbf{Y}_t, \quad t \geq 1,$$

where $\Lambda = \text{diag}(\lambda_1, \ldots, \lambda_d)$ is a $d \times d$ diagonal matrix with $0 < \lambda_s \leq 1$ for $s = 1, \ldots, d$. We should note, for the target process, we use the in-control transformed Gaussian Markov process, $\{\mathbf{Y}_t\}$, to obtain the in-control mean vector and the covariance matrix of $\mathbf{Z}_t$; but for the testing purpose in Phase II, $\{\mathbf{Y}_t^*\}$ instead will be used.

With the recursive property of $\mathbf{Z}_t$ and the fact that $(I - \Lambda)^t + \Lambda\sum_{i=0}^{t-1}(I - \Lambda)^i = I$, Eq. (9) thus can be rewritten as

$$\begin{aligned} \mathbf{Z}_t &= (I - \Lambda)^t\mathbf{Z}_0 + \Lambda\sum_{i=0}^{t-1}(I - \Lambda)^i\mathbf{Y}_{t-i} \\ &= (1 - \Lambda)^t(\mathbf{Z}_0 - \boldsymbol{\mu}_{\mathbf{Y}}) + \Lambda\sum_{i=0}^{t-1}(I - \Lambda)^i(\mathbf{Y}_{t-i} - \boldsymbol{\mu}_{\mathbf{Y}}) \\ (10) \qquad &\quad + \boldsymbol{\mu}_{\mathbf{Y}}, \end{aligned}$$

where the starting value $\mathbf{Z}_0$ is assumed to be a known deterministic quantity usually obtained from historic data. The in-control mean and the covariance matrix of $\mathbf{Z}_t$ are thus obtained by

$$\begin{aligned} E(\mathbf{Z}_t) &= \boldsymbol{\mu}_{\mathbf{Y}} + (I - \Lambda)^t(\mathbf{Z}_0 - \boldsymbol{\mu}_{\mathbf{Y}}), \\ \mathbf{\Sigma}_{\mathbf{Z}_t} &\overset{def.}{=} Cov(\mathbf{Z}_t) \\ (11) \qquad &= \Lambda\sum_{i=0}^{t-1}\sum_{j=0}^{t-1}(I - \Lambda)^i\mathbf{\Sigma}_{\mathbf{Y}}(j - i)(I - \Lambda)^j\Lambda, \end{aligned}$$

respectively. Here, we assume that process always starts with $\mathbf{Z}_0 = \boldsymbol{\mu}_{\mathbf{Y}}$, which implies $E(\mathbf{Z}_t) = \boldsymbol{\mu}_{\mathbf{Y}} = \mathbf{0}$. Also, the in-control covariance matrix of $\mathbf{Z}_t$ is evaluated upon the terms of $\mathbf{\Sigma}_{\mathbf{Y}}(j - i)$ at the lag $j - i$, for $i, j = 0, 1, \ldots, t - 1$. Specifically, for $j \geq i$, $\mathbf{\Sigma}_{\mathbf{Y}}(j - i)$ is obtained from Eq. (7); otherwise from Eq. (8) for $j < i$. The parameters in $\mathbf{\Delta}$ and in $\mathbf{\Sigma}_{\mathbf{Y}}(0)$ (equivalently, in $\mathbf{\Delta}$ and in $\mathbf{\Omega}_{\boldsymbol{\epsilon}}$, see the example given in Eq. (6) for a bivariate case) are estimated upon the transformed in-control Gaussian process $\{\mathbf{Y}_t\}$ using the method in Section 4.

In most situations, without a priori knowledge on the chart smoothing parameters Λ, one usually sets $\lambda_1 = \cdots = \lambda_d = \lambda$, and thus the chart given in Eq. (9) is simplified as

$$(12) \qquad \mathbf{Z}_t = (1 - \lambda)\mathbf{Z}_{t-1} + \lambda\mathbf{Y}_t, \quad t \geq 1.$$

with the in-control covariance matrix simplified by

$$\boldsymbol{\Sigma}_{\mathbf{Z}_t} = \lambda^2 \sum_{i=0}^{t-1}\sum_{j=0}^{t-1}(1-\lambda)^{i+j}\boldsymbol{\Sigma}_{\mathbf{Y}}(j-i). \tag{13}$$

Thus, the recursive format of $\boldsymbol{\Sigma}_{\mathbf{Z}_t}$ in Eq. (13) is obtained as

$$\begin{aligned}\boldsymbol{\Sigma}_{\mathbf{Z}_t} &= (1-\lambda)^2\boldsymbol{\Sigma}_{\mathbf{Z}_{t-1}} + \lambda^2\sum_{i=1}^{t-1}(1-\lambda)^i\boldsymbol{\Sigma}_{\mathbf{Y}}(-i)\\ &\quad +\lambda^2\sum_{j=0}^{t-1}(1-\lambda)^j\boldsymbol{\Sigma}_{\mathbf{Y}}(j).\end{aligned} \tag{14}$$

However, as $t\to\infty$, obtaining $\boldsymbol{\Sigma}_{\mathbf{Z}_t}$ could be time-consuming even using the formula in Eq. (14). For supporting an efficient computation, a proposition is presented as follows:

Proposition 3.1. *Let $\{\mathbf{Y}_t\}$ be a d-variate (weakly) stationary Gaussian Markov process of order one defined in Eq. (5) with the mean $\boldsymbol{\mu}_{\mathbf{Y}} = \mathbf{0}$ and the auto-covariance matrix at the lag h $\boldsymbol{\Sigma}_{\mathbf{Y}}(h) = [\omega_{i,j}(h)]_{i,j=1}^d$. If a multivariate EWMA chart is constructed upon $\mathbf{Y}_t$ by $\mathbf{Z}_t = (1-\lambda)\mathbf{Z}_{t-1} + \lambda\mathbf{Y}_t$ with $0<\lambda\le 1$, then as $t\to\infty$: i) $\boldsymbol{\Sigma}_{\mathbf{Z}_t} = \frac{\lambda}{2-\lambda}\sum_{s=-t+1}^{t-1}(1-\lambda)^{|s|}\boldsymbol{\Sigma}_{\mathbf{Y}}(s)$; ii) $\boldsymbol{\Sigma}_{\mathbf{Z}_t} = \boldsymbol{\Sigma}_{\mathbf{Z}_{t-1}}$ for a large t.*

The proof is given in Appendix. This proposition simplifies the computation procedure for $\boldsymbol{\Sigma}_{\mathbf{Z}_t}$ for a large t. Simply, one can fix $\boldsymbol{\Sigma}_{\mathbf{Z}_t}$ by $\boldsymbol{\Sigma}_{\mathbf{Z}_{t^*}}$ when t reaches an arbitrarily pre-selected large value, say t^*. We also applied this strategy in our simluation section and it works perfectly when $t\ge t^* = 100$.

Following the ideas of Lowry et al. (1992), the chart constructed above for detecting the changes in the location for a multivariate Markov process of order *one* will send a signal when

$$\mathbf{Z}_t'\boldsymbol{\Sigma}_{\mathbf{Z}_t}^{-1}\mathbf{Z}_t > c, \tag{15}$$

where c is a critical value and can be obtained by a scheme that: A pre-defined value ξ for the in-control average run length (ARL) $E(N)$ is given, and the control limit c is determined such that the in-control ARL of the chart is equal to ξ, i.e., $E(N(c)) = \xi$. Usually, this is achieved by simulations. However, we should mention that the chart does not provide any information for which components a change has occurred. Some literatures have proposed the methods for multivariate EWMA chart diagnosis, see Niaki and Abbasi (2005), Reynolds and Cho (2006), Zou et al. (2011), and Jiang et al. (2012), but we will not discuss this here.

4. ESTIMATION FOR IN-CONTROL CHART PARAMETERS

Typically, in quality control, a target process is collected in Phase I for estimating the chart parameters; and in Phase II, the chart constructed upon the estimated parameters is then used to monitor a new observed process. Let the target multivariate (Gaussian or non-Gaussian) Markov process of order *one* be $\{\mathbf{X}_t\}$ with $\mathbf{X}_t = (X_{t,1},\ldots,X_{t,d})'$, for $t = 1,2,\ldots,n$; and let $\mathbf{x}_t$ be realizations of $\mathbf{X}_t$. The key advantage of the proposed semiparametric approach is: The chart can be used for monitoring any non-Gaussian multivariate Markov process in the way analogous to a Gaussian Markov process by transforming a possibly non-Gaussian Markov process $\{\mathbf{X}_t\}$ to a Gaussian Markov process $\{\mathbf{Y}_t\}$ using $Y_{t,s} = \Phi^{-1}(G_s(X_{t,s};\boldsymbol{\beta}_s))$, for $t = 1,\ldots,n$ and $s = 1,\ldots,d$. The in-control chart parameters are then estimated upon this transformed process $\{\mathbf{Y}_t\}$. For this purpose, we evaluate the model using a *multi-stage* maximum likelihood estimation (MSMLE) with two extra conditions: the parameters $\boldsymbol{\beta}_s$ in margin G_s do not also appear in margin $G_{s'}$ for $s\ne s'$, and no cross-equation restrictions on those parameters. Simulation studies (Patton, 2006) indicate that MSMLE is asymptotically less efficient than one-stage MLE, but not great in many cases.

The *first-stage* of MSMLE involves estimating the margin for each time series $\{X_{t,s}\}$, for $s = 1,\ldots,d$, parametrically or nonparametrically. A newly developed semiparametric density estimation approach using the transformed Bernstein polynomial (TBP) prior (Chen et al., 2014) inherits the merits from both parametric and nonparametric models by centering the unknown but need-to-be estimated distribution function at a parametric one as an initial guess; as such, this initial can be adjusted later to approach to the true one if this guess is not correct. The log-likelihood for the margin $G_s(\cdot;\boldsymbol{\beta}_s)$ of $\{X_{t,s}\}$ is given as

$$\begin{aligned} ll(\boldsymbol{\beta}_s) &= \sum_{t=1}^{n}\log g_s(x_{t,s};\boldsymbol{\beta}_s), \quad s = 1,2,\ldots,d,\\ g_s(x_{t,s};\boldsymbol{\beta}_s) &= \sum_{j=1}^{J} w_{J,j}^s b_{J,j}(\Phi(x_{t,s};\mu_s,\sigma_s^2))\phi(x_{t,s};\mu_s,\sigma_s^2),\end{aligned} \tag{16}$$

here $g_s(\cdot;\boldsymbol{\beta}_s)$ is the marginal density associated with $G_s(\cdot;\boldsymbol{\beta}_s)$ and centered at a normal distribution $\Phi(\cdot;\mu_s,\sigma_s^2)$ with its density $\phi(\cdot;\mu_s,\sigma_s^2)$; $b_{J,j}(\cdot)$ is a beta density given as $b_{J,j}(t) = \frac{\Gamma(J+1)}{\Gamma(j)\Gamma(J+1-j)}t^{j-1}(1-t)^{J-j}$ with $\Gamma(\cdot)$ defined as a usual gamma function. By assigning $J\sim p(J)$ independent to the Bernstein coefficients $\mathbf{w}_J^s = (w_{J,1}^s,\ldots,w_{J,J}^s)'$ with $\mathbf{w}_J^s \sim$ Dirichlet$(M\mathbf{1}_J)$, where $\mathbf{1}_J$ is a vector of size J with all elements equal to *one* and the precision parameter $M>0$ controls how likely $x_{t,s}$ follows the centering distribution $\Phi(\cdot;\mu_s,\sigma_s^2)$, we thus center $G_s(\cdot;\boldsymbol{\beta}_s)$ at $\Phi(\cdot;\mu_s,\sigma_s^2)$. Given J, the parameters, $\boldsymbol{\beta}_s$, of G_s is then written as $\boldsymbol{\beta}_s = ([w_{J,j}^s]_{j=1}^J,\mu_s,\sigma_s^2)$. With the smoothness property, $\boldsymbol{\beta}_s$ then can be estimated by maximizing the posterior of $\boldsymbol{\beta}_s$ given J at

$$\begin{aligned}\mathbf{Q}_J = \text{argmax}_{\boldsymbol{\beta}_s}&\sum_{t=1}^{n}\log g_s(x_{t,s};\boldsymbol{\beta}_s)\\ &+\log\pi(\mathbf{w}_J^s)+\log\pi(\mu_s,\sigma_s^2),\end{aligned} \tag{17}$$

for $s = 1, 2, \ldots, d$, here $\pi(\mathbf{w}_J^s)$ and $\pi(\mu_s, \sigma_s^2)$ are the independent priors for $\mathbf{w}_J^s$ and (μ_s, σ_s^2), respectively. Specifically, Eq. (17) is evaluated repeatedly for $J = 1, 2, \ldots, K$, where K is an arbitrarily pre-selected number based on the sample size (Chen et al., 2014) and typically set as $K = 15$. The final J is chosen such that it is the posterior mode of J, and $\hat{\boldsymbol{\beta}}_s$ are then the one corresponding to this J. Although this is not a fully Bayesian approach, it avoids the time-consuming posterior samplings. For more details on the TBP prior and its estimation, see Chen et al. (2014). Note, when $J = 1$ or $w_{J,1} = w_{J,2} = \cdots = w_{J,J} = \frac{1}{J}$ for $J > 1$, we have $G_s(\cdot; \boldsymbol{\beta}_s) \equiv \Phi(\cdot; \mu_s, \sigma_s^2)$. Also, if $G_s(\cdot; \boldsymbol{\beta}_s) \equiv \Phi(\cdot; \mu_s, \sigma_s^2)$ for all $s = 1, \ldots, d$, then the process $\{\mathbf{X}_t\}$ itself is actually a Gaussian Markov process.

With the estimated margins $[\hat{G}_s(\cdot; \hat{\boldsymbol{\beta}}_s)]_{s=1}^d$ from the *first-stage*, then the log-likelihood function used for estimating the copula parameters at the *second-stage* of MSMLE is given as

$$ll(\boldsymbol{\Theta}) = \sum_{t=1}^{n} \log f(\mathbf{x}_t | \mathbf{x}_{t-1}; \boldsymbol{\Theta}), \tag{18}$$

where

$$\begin{aligned} &f(\mathbf{x}_t | \mathbf{x}_{t-1}; \boldsymbol{\Theta}) \\ &\quad = f_1(x_{t,1} | x_{t-1,1}; \rho_1) \times f_2(x_{t,2} | x_{t-1,2}; \rho_2) \\ &\qquad \times \cdots \times f_d(x_{t,d} | x_{t-1,d}; \rho_d) \\ &\qquad \times c_{\boldsymbol{\Omega}}(F_1(x_{t,1} | x_{t-1,1}; \rho_1), \ldots, F_d(x_{t,d} | x_{t-1,d}; \rho_d)) \end{aligned} \tag{19}$$

with

$$\begin{aligned} f_s(x_{t,s} | x_{t-1,s}; \rho_s) &= \hat{g}_s(x_{t,s}; \hat{\boldsymbol{\beta}}_s) \\ &\quad \times c_s(\hat{G}_s(x_{t,s}; \hat{\boldsymbol{\beta}}_s), \hat{G}_s(x_{t-1,s}; \hat{\boldsymbol{\beta}}_s); \rho_s), \end{aligned} \tag{20}$$

for $s = 1, 2, \ldots, d$, here $c_{\boldsymbol{\Omega}}$ is a d-dimensional Gaussian copula density used to evaluate the correlations among the time series, and $\boldsymbol{\Omega} = \boldsymbol{\Omega}_{\boldsymbol{\epsilon}}$ implied by Eq. (5); c_s, for $s = 1, 2, \ldots, d$, is a 2-dimensional Gaussian copula density function with the parameter ρ_s for the autocorrelation of order *one*. The parameters for the whole model in Eq. (18) thus are written as $\boldsymbol{\Theta} = ([\rho_s]_{s=1}^d, \boldsymbol{\Omega}_{\boldsymbol{\epsilon}})$. Note, the parameters which need to be estimated in this stage are actually the copula parameters in $\boldsymbol{\Delta}$ and $\boldsymbol{\Omega}_{\boldsymbol{\epsilon}}$. Thus, $\boldsymbol{\Theta}$ can be estimated equivalently by maximizing the copula log-likelihood function given by

$$\begin{aligned} ll.c(\boldsymbol{\Theta}) &= \sum_{s=1}^{d} \sum_{t=2}^{n} \log c_s(\hat{G}_s(x_{t,s}; \hat{\boldsymbol{\beta}}_s), \hat{G}_s(x_{t-1,s}; \hat{\boldsymbol{\beta}}_s); \rho_s) \\ &\quad + \sum_{i=1}^{n} \log c_{\boldsymbol{\Omega}_{\boldsymbol{\epsilon}}}(F_1(x_{t,1} | x_{t-1,1}; \hat{\boldsymbol{\beta}}_1, \rho_1), \ldots, \\ &\qquad F_d(x_{t,d} | x_{t-1,d}; \hat{\boldsymbol{\beta}}_d, \rho_d)), \end{aligned} \tag{21}$$

here

$$\begin{aligned} &F_s(x_{t,s} | x_{t-1,s}; \hat{\boldsymbol{\beta}}_s, \rho_s) \\ &\quad = \frac{\partial C_s(\hat{G}_s(x_{t,s}; \hat{\boldsymbol{\beta}}_s), \hat{G}_s(x_{t-1,s}; \hat{\boldsymbol{\beta}}_s); \rho_s)}{\partial \hat{G}_s(x_{t-1,s}; \hat{\boldsymbol{\beta}}_s)} \\ &\quad = \frac{\partial C_s(\hat{u}_{t,s}, \hat{u}_{t-1,s}; \rho_s)}{\partial \hat{u}_{t-1,s}} \\ &\quad \stackrel{def.}{=} F_s(\hat{u}_{t,s} | \hat{u}_{t-1,s}; \rho_s) \end{aligned} \tag{22}$$

with $\hat{u}_{t,s} = \hat{G}_s(x_{t,s}; \hat{\boldsymbol{\beta}}_s)$ and $\hat{u}_{t-1,s} = \hat{G}_s(x_{t-1,s}; \hat{\boldsymbol{\beta}}_s)$. Particularly, for a bivariate Gaussian copula, $F_s(\hat{u}_{t,s} | \hat{u}_{t-1,s}; \rho_s) = \Phi(\frac{\Phi^{-1}(\hat{u}_{t,s}) - \rho_s \Phi^{-1}(\hat{u}_{t-1,s})}{\sqrt{1-\rho_s^2}})$; and for $t = 1$, $F_s(x_{t,s} | x_{t-1,s}; \hat{\boldsymbol{\beta}}_s, \rho_s) = \hat{G}_s(x_{t,s}; \hat{\boldsymbol{\beta}}_s)$.

5. SIMULATION STUDIES

In this section, we will examine the ARL of the proposed chart for multivariate Markov processes of order *one*. We will consider two different underlying Markov processes: i) bivariate Gaussian process, and ii) bivariate Student-t (non-Gaussian) process. The multivariate time series can be obtained by

$$\mathbf{y}_t = \boldsymbol{\Delta} \mathbf{y}_{t-1} + \boldsymbol{\epsilon}_t, \tag{23}$$

where $\mathbf{y}_t$ is the realization of $\mathbf{Y}_t$ in Eq. (5), and $\boldsymbol{\epsilon}_t$ is generated from a bivariate Gaussian with mean $\mathbf{0}$ and covariance matrix $\boldsymbol{\Sigma}_{\boldsymbol{\epsilon}}$. To start this recursively data-generating process, we have $\mathbf{y}_0$ from a bivariate Gaussian with mean $\mathbf{0}$ and covariance matrix $\boldsymbol{\Sigma}_{\mathbf{Y}}(0)$. We should note: Given the $\boldsymbol{\Delta}$ and the correlation matrix $\boldsymbol{\Omega}_{\boldsymbol{\epsilon}}$ of $\boldsymbol{\epsilon}$, from Eq. (6) and $\boldsymbol{\Sigma}_{\boldsymbol{\epsilon}} = \boldsymbol{\Sigma}_{\mathbf{Y}}(0) - \boldsymbol{\Delta}\boldsymbol{\Sigma}_{\mathbf{Y}}(0)\boldsymbol{\Delta}'$, the both $\boldsymbol{\Sigma}_{\mathbf{Y}}(0)$ and $\boldsymbol{\Sigma}_{\boldsymbol{\epsilon}}$ can be obtained easily. Thus, in this section, we only consider several combinations of $\boldsymbol{\Delta}$ and $\boldsymbol{\Omega}_{\boldsymbol{\epsilon}}$. Also, the realizations in the time series $\{X_{t,s}\}$, for $s = 1, 2$, can be obtained by $x_{t,s} = G_s^{-1}(\Phi(y_{t,s}); \boldsymbol{\beta}_s)$, where under the scenario i): $G_s^{-1}(\cdot; \boldsymbol{\beta}_s)$ is the quantile function of a Gaussian with $\boldsymbol{\beta}_s = (\mu_s = 0, \sigma_s^2 = 1)$ for in-control status and $\boldsymbol{\beta}_s = (\mu_s = 0 + \delta\sigma_s, \sigma_s^2 = 1)$ for out of control; and under the scenario ii): $G_s^{-1}(\cdot; \boldsymbol{\beta}_s)$ is the quantile function of a Student-t with $\boldsymbol{\beta}_s$ as the degree of freedom 10 for in-control status and $x_{t,s} = G_s^{-1}(\Phi(y_{t,s}); \boldsymbol{\beta}_s) + \delta\sqrt{\frac{\boldsymbol{\beta}_s}{\boldsymbol{\beta}_s - 2}}$ for out of control. δ is taken from the set of $\{0, 0.5, 1, 1.5, 2, 2.5, 3\}$ and we include $\delta = 0$ for in control purpose. For both scenarios, we arbitrarily shift the mean of X_1 and leave X_2 always in-control. The chart smoothing parameters are set as $\lambda_1 = \lambda_2 = \lambda = 0.1$ and the control limit c is obtained by simulation with the in-control ARL equal to 200, i.e., $E(N(c)) = 200$. The simulation results are reported in Table 1, Table 2, and Table 3.

In Table 1, the $\boldsymbol{\Delta}$ is a *zero* matrix, which means that $\mathbf{Y}_t$ is independent of $\mathbf{Y}_{t-1}$. The chart thus performs in a similar way to the traditional charts in which observations are stochastically independent. We can observe that the simulated control limit c (9.21) from the proposed chart for bivariate Gaussian is larger than the one reported from Lowry et al. (1992) since we estimate the parameters for chart and

Table 1. bivariate process with $\lambda = 0.1$ and the in-control ARL $E(N) = 200$

Scenario i): Bivariate Gaussian Process with $\lambda = 0.1$ and In-Control $ARL = 200$									
$\boldsymbol{\Delta}$	$\boldsymbol{\Omega_\epsilon}$	c	δ						
			0.0	0.5	1.0	1.5	2.0	2.5	3.0
$\begin{pmatrix}0.0 & 0.0\\0.0 & 0.0\end{pmatrix}$	$\begin{pmatrix}1.0 & 0.0\\0.0 & 1.0\end{pmatrix}$	9.21	200.95	22.09	6.49	3.37	2.16	1.64	1.30
$\begin{pmatrix}0.0 & 0.0\\0.0 & 0.0\end{pmatrix}$	$\begin{pmatrix}1.0 & 0.2\\0.2 & 1.0\end{pmatrix}$	9.21	200.18	22.13	6.97	4.06	2.60	1.94	1.57
$\begin{pmatrix}0.0 & 0.0\\0.0 & 0.0\end{pmatrix}$	$\begin{pmatrix}1.0 & 0.5\\0.5 & 1.0\end{pmatrix}$	9.21	199.32	21.74	6.39	3.32	2.15	1.61	1.28
$\begin{pmatrix}0.0 & 0.0\\0.0 & 0.0\end{pmatrix}$	$\begin{pmatrix}1.0 & 0.8\\0.8 & 1.0\end{pmatrix}$	9.21	199.90	20.96	6.53	4.01	2.33	1.10	1.02
Scenario ii): Bivariate Student-t Process with $\lambda = 0.1$ and In-Control $ARL = 200$									
$\boldsymbol{\Delta}$	$\boldsymbol{\Omega_\epsilon}$	c	δ						
			0.0	0.5	1.0	1.5	2.0	2.5	3.0
$\begin{pmatrix}0.0 & 0.0\\0.0 & 0.0\end{pmatrix}$	$\begin{pmatrix}1.0 & 0.0\\0.0 & 1.0\end{pmatrix}$	9.51	200.84	23.40	7.57	4.46	2.82	2.07	1.61
$\begin{pmatrix}0.0 & 0.0\\0.0 & 0.0\end{pmatrix}$	$\begin{pmatrix}1.0 & 0.2\\0.2 & 1.0\end{pmatrix}$	9.51	200.60	23.97	7.30	4.25	2.78	2.00	1.55
$\begin{pmatrix}0.0 & 0.0\\0.0 & 0.0\end{pmatrix}$	$\begin{pmatrix}1.0 & 0.5\\0.5 & 1.0\end{pmatrix}$	9.51	199.59	22.49	6.70	3.49	2.25	1.70	1.33
$\begin{pmatrix}0.0 & 0.0\\0.0 & 0.0\end{pmatrix}$	$\begin{pmatrix}1.0 & 0.8\\0.8 & 1.0\end{pmatrix}$	9.51	199.54	20.57	6.69	4.01	2.39	1.13	1.02

Table 2. bivariate process with $\lambda = 0.1$ and the in-control ARL $E(N) = 200$

Scenario i): Bivariate Gaussian Process with $\lambda = 0.1$ and In-Control $ARL = 200$									
$\boldsymbol{\Delta}$	$\boldsymbol{\Omega_\epsilon}$	c	δ						
			0.0	0.5	1.0	1.5	2.0	2.5	3.0
$\begin{pmatrix}0.8 & 0.0\\0.0 & 0.2\end{pmatrix}$	$\begin{pmatrix}1.0 & 0.0\\0.0 & 1.0\end{pmatrix}$	8.60	200.03	126.75	51.83	22.87	10.93	5.47	3.12
$\begin{pmatrix}0.8 & 0.0\\0.0 & 0.2\end{pmatrix}$	$\begin{pmatrix}1.0 & 0.2\\0.2 & 1.0\end{pmatrix}$	8.50	200.02	125.28	49.95	22.49	10.40	5.44	2.96
$\begin{pmatrix}0.8 & 0.0\\0.0 & 0.2\end{pmatrix}$	$\begin{pmatrix}1.0 & 0.5\\0.5 & 1.0\end{pmatrix}$	8.50	199.99	108.27	38.38	17.65	7.91	4.05	2.36
$\begin{pmatrix}0.8 & 0.0\\0.0 & 0.2\end{pmatrix}$	$\begin{pmatrix}1.0 & 0.8\\0.8 & 1.0\end{pmatrix}$	8.15	200.16	92.21	26.51	10.92	5.25	2.68	1.71
Scenario ii): Bivariate Student-t Process with $\lambda = 0.1$ and In-Control $ARL = 200$									
$\boldsymbol{\Delta}$	$\boldsymbol{\Omega_\epsilon}$	c	δ						
			0.0	0.5	1.0	1.5	2.0	2.5	3.0
$\begin{pmatrix}0.8 & 0.0\\0.0 & 0.2\end{pmatrix}$	$\begin{pmatrix}1.0 & 0.0\\0.0 & 1.0\end{pmatrix}$	9.00	200.95	136.25	60.13	25.39	11.64	6.37	3.41
$\begin{pmatrix}0.8 & 0.0\\0.0 & 0.2\end{pmatrix}$	$\begin{pmatrix}1.0 & 0.2\\0.2 & 1.0\end{pmatrix}$	9.00	200.57	135.08	60.15	24.81	11.52	6.02	3.48
$\begin{pmatrix}0.8 & 0.0\\0.0 & 0.2\end{pmatrix}$	$\begin{pmatrix}1.0 & 0.5\\0.5 & 1.0\end{pmatrix}$	9.00	200.19	113.41	47.21	18.44	8.85	4.66	2.63
$\begin{pmatrix}0.8 & 0.0\\0.0 & 0.2\end{pmatrix}$	$\begin{pmatrix}1.0 & 0.8\\0.8 & 1.0\end{pmatrix}$	8.25	200.82	96.74	31.96	11.70	5.75	2.87	1.83

thus more variabilities are added, which also gives the reason that the value of c (9.51) is even larger for non-Gaussian processes since more estimated parameters are included. However, the proposed chart is invariant for different $\boldsymbol{\Omega_\epsilon}$ when data is collected independently, see Table 1, but this is just a particular scenario. In other situations where data are collected in the time order, the control limits c may vary for different combinations of $\boldsymbol{\Delta}$ and $\boldsymbol{\Omega_\epsilon}$. But, in Table 2 and Table 3, we can see when the correlations in $\boldsymbol{\Omega_\epsilon}$ are small or moderate, the limits c may stay the same or not change too much. But as the correlations go up, the limits c decrease quickly for both Gaussian and non-Gaussian underlying processes. We also observed that the greater the values of the diagonal elements in $\boldsymbol{\Delta}$, the greater is the extension of the regions

Table 3. bivariate process with $\lambda = 0.1$ and the in-control ARL $E(N) = 200$

Scenario i): Bivariate Gaussian Process with $\lambda = 0.1$ and In-Control $ARL = 200$									
$\boldsymbol{\Delta}$	$\boldsymbol{\Omega_\epsilon}$	c	δ						
			0.0	0.5	1.0	1.5	2.0	2.5	3.0
$\begin{pmatrix} -0.4 & 0.0 \\ 0.0 & 0.6 \end{pmatrix}$	$\begin{pmatrix} 1.0 & 0.0 \\ 0.0 & 1.0 \end{pmatrix}$	9.30	200.43	13.66	4.75	2.83	2.07	1.70	1.46
$\begin{pmatrix} -0.4 & 0.0 \\ 0.0 & 0.6 \end{pmatrix}$	$\begin{pmatrix} 1.0 & 0.2 \\ 0.2 & 1.0 \end{pmatrix}$	9.25	199.30	12.86	4.67	2.78	2.03	1.68	1.44
$\begin{pmatrix} -0.4 & 0.0 \\ 0.0 & 0.6 \end{pmatrix}$	$\begin{pmatrix} 1.0 & 0.5 \\ 0.5 & 1.0 \end{pmatrix}$	9.25	199.66	11.01	4.22	2.58	1.91	1.60	1.40
$\begin{pmatrix} -0.4 & 0.0 \\ 0.0 & 0.6 \end{pmatrix}$	$\begin{pmatrix} 1.0 & 0.8 \\ 0.8 & 1.0 \end{pmatrix}$	8.30	199.03	9.38	3.74	2.35	1.81	1.53	1.33
Scenario ii): Bivariate Student-t Process with $\lambda = 0.1$ and In-Control $ARL = 200$									
$\boldsymbol{\Delta}$	$\boldsymbol{\Omega_\epsilon}$	c	δ						
			0.0	0.5	1.0	1.5	2.0	2.5	3.0
$\begin{pmatrix} -0.4 & 0.0 \\ 0.0 & 0.6 \end{pmatrix}$	$\begin{pmatrix} 1.0 & 0.0 \\ 0.0 & 1.0 \end{pmatrix}$	9.65	200.16	14.48	4.92	2.87	2.143	1.75	1.54
$\begin{pmatrix} -0.4 & 0.0 \\ 0.0 & 0.6 \end{pmatrix}$	$\begin{pmatrix} 1.0 & 0.2 \\ 0.2 & 1.0 \end{pmatrix}$	9.60	199.91	13.42	4.69	2.86	2.12	1.74	1.51
$\begin{pmatrix} -0.4 & 0.0 \\ 0.0 & 0.6 \end{pmatrix}$	$\begin{pmatrix} 1.0 & 0.5 \\ 0.5 & 1.0 \end{pmatrix}$	9.60	199.87	11.42	4.23	2.69	1.99	1.69	1.47
$\begin{pmatrix} -0.4 & 0.0 \\ 0.0 & 0.6 \end{pmatrix}$	$\begin{pmatrix} 1.0 & 0.8 \\ 0.8 & 1.0 \end{pmatrix}$	8.60	199.16	9.94	3.80	2.43	1.88	1.60	1.37

towards the direction of the variables affected by those diagonal elements. Consequently, the ARLs in Table 3 are much smaller than the ones reported in Table 2 for out-of-control. A similar phenomenon was also observed in the Monte Carlo studies by Kramer and Schmid (1997). In summary, the proposed chart works well under the simulated situations for both Gaussian and non-Gaussian Markov processes of order *one*. In addition, with AMD Athlon 4 CPU@498.26 MHz (a very old laptop), the recorded CPU time for obtaining the control limit c by simulation with 5000 replicates is 452 seconds.

6. A REAL EXAMPLE

In the following, an example is presented making use of data from Quarterly Gross Domestic Product (QGDP). Briefly, QGDP is the monetary value of all the finished goods and services produced within a country's borders calculated on a quarterly basis, and it is a broad measurement of a nation's overall economic activity. The data called "qgdp" could be found in the R package **MTS** (Tsay, 2015) and we consider the quarterly gross domestic products of United Kingdom (UK), Canada (CA), and the United States (US) in the time period from the first quarter of 1980 to the second quarter of 2011, i.e. the total of 126 quarters during this time period. We let S_{it} represent the gross domestic product of the ith country with $i = 1$ for UK, $i = 2$ for CA, and $i = 3$ for US at the tth quarter, for $t = 1, \ldots, 126$. Practically, one is usually interested in the transformed data which is the log ratio of two adjacent quarter gross domestic products, denoted as $X_{it} = \log(S_{it}/S_{i,t-1})$ for $t = 2, \ldots, 126$. The total

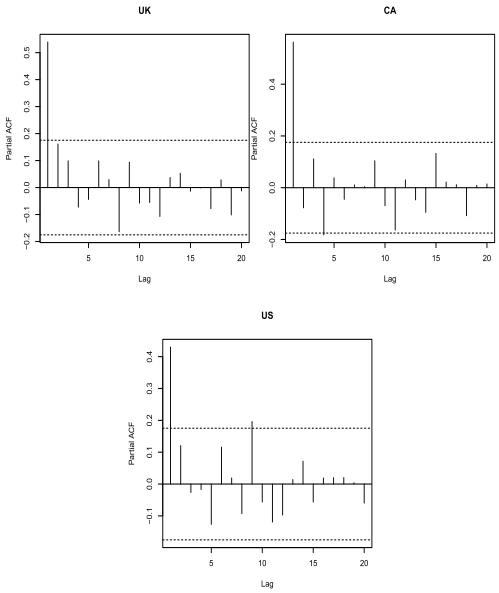

Figure 1. Partial Autocorrelations.

sample size thereafter is $n = 125$. To examine whether this data set is suitable to the proposed chart, we further investigated the partial autocorrelations of those 3 time series, see Figure 1. Apparently, it is reasonable to use our method to fit a copula transformed multivariate Markov process of order *one* given as the follows,

$$\mathbf{Y}_t = \boldsymbol{\Delta}\mathbf{Y}_{t-1} + \boldsymbol{\epsilon}_t^*, \tag{24}$$

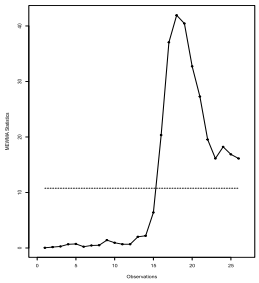

Figure 2. QGDP: Fitted Chart From MEWMA.

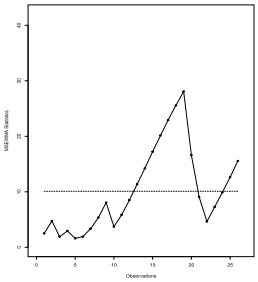

Figure 3. QGDP: Fitted Chart From MSEWMA.

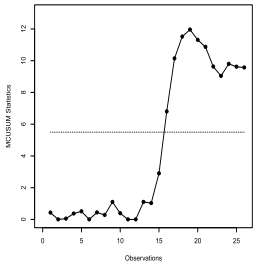

Figure 4. QGDP: Fitted Chart From MCUSUM.

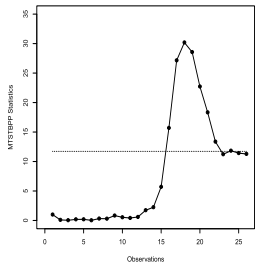

Figure 5. QGDP: Fitted Chart From MTSTBPP.

where $\mathbf{Y}_t = (Y_{1t}, Y_{2t}, Y_{3t})'$ and $Y_{it} = \Phi^{-1}(\hat{G}_i(X_{it}; \hat{\boldsymbol{\beta}}_i))$, for $i = 1, 2, 3$, and $G_i(\cdot; \boldsymbol{\beta}_i)$ is estimated marginally via the method MSMLE given in Section 4 from Phase I.

For the target process, we took the first 99 transformed observations, i.e. the time period from the first quarter of 1980 to the fourth quarter of 2004. The model given in Eq. (24) was evaluated using the copula log-likelihood in Eq. (21), and we obtained the estimated parameters as

$$\widehat{\boldsymbol{\Delta}} = \begin{pmatrix} 0.433 & 0 & 0 \\ 0 & 0.448 & 0 \\ 0 & 0 & 0.154 \end{pmatrix},$$

$$\widehat{\boldsymbol{\Sigma}_{\mathbf{Y}}}(0) = \begin{pmatrix} 1 & -0.070 & 0.069 \\ -0.070 & 1 & 0.472 \\ 0.069 & 0.472 & 1 \end{pmatrix}.$$

Thus by $\widehat{\boldsymbol{\Sigma}_{\boldsymbol{\epsilon}^*}} = \widehat{\boldsymbol{\Sigma}_{\mathbf{Y}}}(0) - \widehat{\boldsymbol{\Delta}}\widehat{\boldsymbol{\Sigma}_{\mathbf{Y}}}(0)\widehat{\boldsymbol{\Delta}}'$,

$$\widehat{\boldsymbol{\Sigma}_{\boldsymbol{\epsilon}^*}} = \begin{pmatrix} 0.812 & -0.056 & 0.064 \\ -0.056 & 0.799 & 0.439 \\ 0.064 & 0.439 & 0.976 \end{pmatrix}.$$

The corresponding simulated control limit c is 11.72 for the common smoothing parameter $\lambda = 0.1$ and the in-control ARL $E(N(c)) = 200$.

Assuming this model we run a control chart over the next 26 transformed observations, i.e. the time period from the first quarter of 2005 to the send quarter of 2011. Our aim is to detect changes in the log ratio of two adjacent quarter gross domestic products, which further can be used to assess a nation's overall economic activity for measuring a nation's economic growth or decline, as well as for determining if an economy is in recession. The proposed control chart (MTSTBPP) is plotted along with the charts constructed from the multivariate EWMA (MEWMA) from Lowry et al. (1992), the multivariate sign EWMA (MSEWMA) from Zou and Tsung (2011), and the multivariate CUSUM (MCUSUM) from Tartakovsky et al. (2014), see Figure 2, Figure 3, Figure 4, and Figure 5. MEWMA and MSEWMA assume the independence of observations with the former having an additional normality assumption on the monitored process and the latter relaxing this normality assumption by its nonparametric setup. In contrast, our proposed MTSTBPP chart relaxes the both assumptions by: 1) using the transformed Bernstein polynomial prior (TBPP) for modeling Gaussian or non-Gaussian margins, and 2) fitting copulas to account for the dependence structure of the monitored process. Seemly, the fitted charts from MEWMA, MCUSUM, and MTSTBPP control schemes are quite similar to each other. For example, starting from the 16th observations, the out-of-control was observed, which means there is a big change in the log ratio of GDPs between the third quarter and the fourth quarter of 2008. It is well known that the global financial crisis or called the 2008–2009 financial crisis occurred in this time period, and this crisis is considered by many economists to have been the worst financial crisis since the Great Depression of the 1930s. This crisis obviously has an impact on GDPs in many countries including UK, CA, and US. However, compared to MEWMA and MCUSUM charts, the last four observations in MTSTBPP chart, i.e. the time period from the second quarter of 2010 to the second quarter of 2011, are in-control even if they are

quite close to the control border, which corresponds to the observed fact that this great global recession was ended in early 2010s. MSEWMA chart performs a little bit difference since it starts to report the out-of-control status at the first quarter of 2008, which is earlier compared to other three charts; it also shows that the global economy was getting better at the last quarter of 2009, but then worse again at the first quarter of 2011.

7. CONCLUSIONS

In this paper, we presented a semiparametric control scheme for multivariate Markov processes of order *one*. The original multivariate autocorrelated processes are transformed to the ones in which the marginal information of the monitored characteristics are separate out from their dependence structures with the latter then characterized by copulas. Meanwhile, copulas are also used for estimating the correlations across them. To monitor Gaussian or non-Gaussian distributed characteristics marginally, we utilize the transformed Bernstein polynomial priors (Chen et al., 2014) to allow initial parametric guesses on the monitored characteristics; then by adding more details via data, departures from initial guesses will be captured and used for adjusting the initials to obtain robust estimations. Gaussian copulas are used for evaluating the dependence structure among the characteristics and their autocorrelations. It is shown that the proposed chart performs much better than the traditional charts for stochastically dependent processes as the traditional ones frequently trigger signals even if there are actually no operation problems.

Despite the successful analysis presented in this paper, the author must point out that the proposed model is currently designed to model Markov processes of order *one*. In principle, the model can be extended to modeling Markov processes of any finite order. We should note that the proposed model has an additional appealing feature when it is used for modeling higher order Markov process for each time series, i.e., each of those time series depends on only one dimension margin estimation and its autocorrelations will be separately evaluated by copulas. Furthermore, although the proposed model can theoretically cooperate with different types of copulas for various dependence structures, we only investigate the Gaussian copulas in this paper for the both autocorrelations within the time series and correlations across them since the Gaussian dependence structure is the most commonly used one in multivariate Markov processes. But for different types of data, such as the data collected from the stock market, the Student-t copulas or the skewed Student-t copulas will be more appropriate in the sense that the tail dependence information can be evaluated.

APPENDIX

Proof. By Eq. (11) and Eq. (13), we obtain

$$
\begin{aligned}
\boldsymbol{\Sigma}_{\mathbf{Z}_t} &= \lambda^2 \sum_{i=0}^{t-2} \sum_{j=i+1}^{t-1} (1-\lambda)^{i+j} \boldsymbol{\Delta}^{j-i} \boldsymbol{\Sigma}_{\mathbf{Y}}(0) \\
&\quad + \lambda^2 \sum_{i=1}^{t-1} \sum_{j=0}^{i-1} (1-\lambda)^{i+j} \boldsymbol{\Sigma}_{\mathbf{Y}}(0) \boldsymbol{\Delta}^{i-j} \\
&\quad + \lambda^2 \sum_{i=0}^{t-1} (1-\lambda)^{2i} \boldsymbol{\Sigma}_{\mathbf{Y}}(0) \\
&= \lambda^2 \sum_{i=0}^{t-2} \sum_{j=i+1}^{t-1} (1-\lambda)^{i+j} \boldsymbol{\Sigma}_{\mathbf{Y}}(j-i) \\
&\quad + \lambda^2 \sum_{i=1}^{t-1} \sum_{j=0}^{i-1} (1-\lambda)^{i+j} \boldsymbol{\Sigma}_{\mathbf{Y}}(-(i-j)) \\
&\quad + \lambda^2 \sum_{i=0}^{t-1} (1-\lambda)^{2i} \boldsymbol{\Sigma}_{\mathbf{Y}}(0) \\
&= \lambda^2 \sum_{s=-t+1}^{t-1} \boldsymbol{\Sigma}_{\mathbf{Y}}(s) \sum_{\nu=max(0,-s)}^{min(t-1,t-1-s)} (1-\lambda)^{s+2\nu} \\
&= \frac{\lambda}{2-\lambda} \sum_{s=-t+1}^{t-1} (1-\lambda)^{|s|} \boldsymbol{\Sigma}_{\mathbf{Y}}(s) \\
&\quad - \frac{\lambda(1-\lambda)^{2t}}{2-\lambda} \sum_{s=-t+1}^{t-1} (1-\lambda)^{-|s|} \boldsymbol{\Sigma}_{\mathbf{Y}}(s), \qquad (25)
\end{aligned}
$$

and as $t \to \infty$, the second term in the right hand side of Eq. (25) *approaches* to *zero*, and thus we have

$$
\boldsymbol{\Sigma}_{\mathbf{Z}_t} = \frac{\lambda}{2-\lambda} \sum_{s=-t+1}^{t-1} (1-\lambda)^{|s|} \boldsymbol{\Sigma}_{\mathbf{Y}}(s), \quad \text{as } t \to \infty. \qquad (26)
$$

Also, we noticed that as $t \to \infty$, when $s = t-1$ or $s = -t+1$, $\sum_{\nu=max(0,-s)}^{min(t-1,t-1-s)} (1-\lambda)^{s+2\nu} = 0$ since $0 < \lambda \leq 1$. It implies for a large t, the term $(1-\lambda)^{s+2\nu}$ almost has no contribution to $\boldsymbol{\Sigma}_{\mathbf{Z}_t}$. Thus, we obtain $\boldsymbol{\Sigma}_{\mathbf{Z}_t} = \boldsymbol{\Sigma}_{\mathbf{Z}_{t-1}}$ as $t \to \infty$. □

ACKNOWLEDGEMENTS

Chen's research was supported in part by 2015 Research Grants Committee, the University of Alabama.

Received 12 May 2016

REFERENCES

Albers, W. and Kallenberg, W. (2004). Empirical non-parametric control charts: estimation effects and corrections. *Journal of Applied Statistics*, **31**, 345–360. MR2061387

Alwan, L. and Roberts, H. (1988). Time-series modeling for statistical process control. *Journal of Business and Economic Statistics*, **6**, 87–95.

Chakraborti, S. and Eryilmaz, S. (2007). A nonparametric Shewhart-type signed-rank control charts based on runs. *Communications in Statistics-Simulation and Computation*, **36**, 335–356. MR2370905

Chan, L. and Li, G. (1994). A multivariate control chart for detecting linear trends. *Communications in Statistics-Simulation and Computation*, **23**, 997–1012. MR1309947

Charnes, J. (1995). Tests for special causes with multivariate autocorrelated data. *Computers and Operational Research*, **22**, 443–453.

Chen, X. and Fan, Y. (2006). Estimation of copula-based semiparametric time series models. *Journal of Econometrics*, **130**, 307–335. MR2211797

Chen, Y. (2015). A new type of Bayesian nonparametric control charts for individual measurements. *Journal of Statistical Theory and Practice*, accepted. MR3453038

Chen, Y. and Hanson, T. (2014). Bayesian nonparametric k-sample tests for censored and uncensored data. *Computational Statistics and Data Analysis*, **71**, 335–346. MR3131974

Chen, Y. and Hanson, T. (2016+). Nonparametric regression control charts. *Statistical Methods and Applications*, submitted. MR3453038

Chen, Y., Hanson, T., and Zhang, J. (2014). Accelerated hazards model based on parametric families generalized with Bernstein polynomials. *Biometrics*, **70**, 192–201. MR3251680

Chen, Y., Sun, M., and Hanson, T. (2016+). Nonparametric multivariate Polya tree EWMA control chart for process changepoint detection. *Journal of Nonparametric Statistics*, submitted.

Crosier, R. (1988). Multivariate generalizations of cumulative sum quality-control schemes. *Technometrics*, **30**, 291–303. MR0959530

Crowder, S. (1987). A simple method for studying run length distributions of exponentially weighted moving average charts. *Technometrics*, **29**, 401–407. MR0918526

Crowder, S. (1989). Design of exponentially weighted moving average schemes. *Journal of Quality Technology*, **21**, 155–162.

Duncan, A. (1965). *Quality Control and Industrial Statistics*. Homewood, IL: R. D. Irwin. MR0101600

Hanson, T. (2006). Inference for mixture of finite Polya tree models. *Journal of the American Statistical Association*, **101**, 1548–1565. MR2279479

Hawkins, D. and Olwell, D. (1998). *Cumulative Sum Charts and Charting for Quality Improvement*. Springer, New York. MR1601506

Hotelling, H. (1947). Multivariate Quality Control – Illustrated by the Air Testing of Sample Bombsights in *Techniques of Statistical Analysis*. McGraw-Hill, New York, 111–184.

Jiang, W., Wang, K., and Tsung, F. (2012). A variable-selection-based multivariate EWMA chart for process monitoring and diagnosis. *Journal of Quality Technology*, **44**, 209–230.

Kalgonda, A. and Kulkarni, S. (2004). Multivariate quality control chart for autocorrelated processes. *Journal of Applied Statistics*, **31**, 317–327. MR2061386

Kramer, H. and Schmid, W. (1997). EWMA charts for multivariate time series. *Sequential Analysis*, **16**, 131–154. MR1456981

Lowry, C., Woodall, W., Champ, C., and Rigdon, S. (1992). A multivariate exponentially weighted moving average control chart. *Technometrics*, **34**, 46–53.

Lu, C. and Reynolds, M. (1995). Control charts based on residuals for monitoring autocorrelated processes. *Technical Report, Dept. of Statistics, Virginia Polytechnic Institute and State University*. Blacksburg (VA).

Lucas, J. and Saccucci, M. (1990). Exponentially weighted moving average control schemes: properties and enhancements (with discussion). *Technometrics*, **32**, 1–29. MR1050277

Martin, K. and Petr, K. (2012). The usage of time series control charts for financial process analysis. *Journal of Competitiveness*, **4**, 29–45.

Montgomery, D. and Mastrangelo, C. (1991). Some statistical process control methods for autocorrelated data. *Journal of Quality Technology*, **23**, 179–204.

Moskvina, V. and Zhigljavsky, A. (2003). An algorithm based on singular spectrum analysis for change-point detection. *Communications in Statistics – Simulation and Computation*, **32**, 319–352. MR1983338

Niaki, S. and Abbasi, B. (2005). Fault diagnosis in multivariate control charts using artificial neural networks. *Quality and Reliability Engineering International*, **21**, 825–840.

Page, E. (1954). Continuous inspection schemes. *Biometrika*, **41**, 100–115. MR0088850

Patton, A. (2006). Estimation of multivariate models for time series of possibly different lengths. *Journal of Applied Econometrics*, **21**, 147–173. MR2226593

Pignatiello, J. and Runger, G. (1990). Comparisons of multivariate CUSUM charts. *Journal of Quality Technology*, **22**, 173–186.

Reynolds, M. and Cho, G. (2006). Multivariate control charts for monitoring the mean vector and covariance matrix. *Journal of Quality Technology*, **38**, 230–253.

Roberts, S. (1959). Control chart tests based on geometric moving averages. *Technometrics*, **1**, 239–250.

Ross, G. and Adams, N. (2012). Two nonparametric control charts for detecting arbitrary distribution changes. *Journal of Quality Technology*, **44**, 102–116.

Tartakovsky, A., Nikiforov, I., and Basseville, M. (2014). *Sequential Analysis: Hypothesis Testing and Changepoint Detection*. CRC Press. MR3241619

Theodossiou, P. (1993). Predicting shift in the mean of a multivariate time series process: an application in predicting business failures. *Journal of the American Statistical Association*, **88**, 441–449.

Tsay, R. (2015). All-purpose toolkit for analyzing multivariate time series (MTS) and estimation multivariate volatility models. *R package*.

Shewhart, W. (1931). *Economic Control of Quality of Manufactured Product*. Princeton, NJ: Van Nostrand.

Sklar, A. (1959). Fonctions de répartition à n dimensions et leurs marges. *Publications de l'Institut de Statistique de l'Université de Paris*, **8**, 229–231. MR0125600

Willemain, T. and Runger, G. (1996). Designing control charts using an empirical reference distribution. *Journal of Quality Technology*, **28**, 31–38.

Woodall, W. and Ncube, M. (1985). Multivariate CUSUM quality control procedures. *Technometrics*, **27**, 285–292. MR0797567

Zou, C., Jiang, W., and Tsung, F. (2011). A lasso-based diagnostic framework for multivariate statistical process control. *Technometrics*, **53**, 297–309. MR2867503

Zou, C. and Tsung, F. (2011). A multivariate sign EWMA control chart. *Technometrics*, **53**, 84–97. MR2791949

Yuhui Chen
Assistant Professor
Department of Mathematics
The University of Alabama
Tuscaloosa, AL
USA
E-mail address: ychen164@ua.edu